fishes

MDPI

Article

Population Structure of the European Seabass (*Dicentrarchus labrax*) in the Atlantic Iberian Coastal Waters Inferred from Body Morphometrics and Otolith Shape Analyses

Rafael Gaio Kulzer [1,2], Rodolfo Miguel Silva [2,3], Ana Filipa Rocha [4], João Soares Carrola [4,5], Rosária Catarino Seabra [2,3], Eduardo Rocha [2,3], Karim Erzini [1,6] and Alberto Teodorico Correia [2,3,*]

1 Faculty of Sciences and Technology (FCT), University of Algarve (UALG), Campus de Gambelas, 8005-139 Faro, Portugal
2 Interdisciplinary Centre of Marine and Environmental Research (CIIMAR/CIMAR), Terminal de Cruzeiros do Porto de Leixões, Avenida General Norton de Matos S/N, 4450-208 Matosinhos, Portugal
3 School of Medicine and Biochemical Sciences (ICBAS), University of Porto (UP), Rua Jorge Viterbo Ferreira 228, 4050-313 Porto, Portugal
4 School of Life and Environmental Sciences (ECVA), University of Trás-os-Montes and Alto Douro (UTAD), Quinta de Prados, 5000-801 Vila Real, Portugal
5 Centre for the Research and Technology of Agro-Environmental and Biological Sciences (CITAB), Institute for Innovation, Capacity Building and Sustainability of Agri-Food Production (Inov4Agro), University of Trás-os-Montes and Alto Douro (UTAD), Quinta de Prados, 5000-801 Vila Real, Portugal
6 Centre of Marine Sciences (CCMAR/CIMAR), University of Algarve (UALG), Campus de Gambelas, 8005-139 Faro, Portugal
* Correspondence: atcorreia@icbas.up.pt

Abstract

The European seabass (*Dicentrarchus labrax*) is one of the most emblematic coastal fish species in the Northeast Atlantic, with high commercial value for fisheries and aquaculture, and importance for sport and recreational fishing. Despite its socio-economic importance, the Iberian divisions, Cantabrian Sea (8c) and the Atlantic Iberian waters (9a), defined by the International Council for the Exploration of the Sea (ICES), lack stock delimitation data. Moreover, this species is missing basic biological information, a seasonal reproductive fishing ban, and the annual landings in this region are more than double the levels recommended by ICES. To investigate the population structure of *D. labrax* in these areas, 140 adult individuals (36–51 cm of total length) were collected between January and March 2025 in three locations along the Atlantic coast of the Iberian Peninsula: Avilés (n = 47), Peniche (n = 48), and Lagos (n = 45). Fish from each location were analyzed for body geometric morphometrics (truss network) and otolith shape contour (Elliptical Fourier Descriptors). Data were evaluated using univariate and multivariate tests to assess spatial differences and reclassification success among locations. Results revealed regional differences using body morphometry and otolith shape analyses. The overall reclassification success was 68% for truss networking, 51% for otolith shape, and 65% when both methods were combined. Despite the observed differences, the absence of clear, isolated populations supports the ICES definition of a single, though not homogeneous, European seabass stock in the Atlantic Iberian coastal waters. Nevertheless, individuals from Avilés exhibited distinctive morphometric patterns and otolith shapes, suggesting possible adaptations to local selective pressures in slightly different environments. Further studies integrating genetic tools, otolith chemistry, parasitic fauna and telemetry analyses, as well as other fish samples from adjacent areas such as the Bay of Biscay, are recommended to achieve a more comprehensive understanding of the population structure and migration patterns of this key species in the Atlantic Iberian coastal waters.

Academic Editor: Jian Yang

Received: 7 November 2025
Revised: 18 December 2025
Accepted: 24 December 2025
Published: 27 December 2025

Keywords: demersal fish; stock delineation; natural tags; truss networking; elliptical Fourier descriptors

Key Contribution: The population structure of *Dicentrarchus labrax* along the Atlantic Iberian coast was assessed using body morphometrics and otolith shape analyses, revealing regional phenotypic differences with reclassification success rates up to 68%. Results support a single but heterogeneous stock, with indications of local adaptation in Avilés fish and the need for complementary research.

1. Introduction

The European seabass (*Dicentrarchus labrax*) is a widely distributed coastal fish that inhabits most of the northeastern Atlantic, from Scotland and Scandinavia to the Canary Islands and the Atlantic coast of Morocco, and also occurs throughout the Baltic, Mediterranean and Black Seas [1–3]. Although primarily marine, adult *D. labrax* exhibits remarkable ecological plasticity, tolerating a broad range of salinities from hyperhaline to brackish waters with individuals that may migrate several tens of kilometres upstream into rivers [4] and can even remain in freshwater habitats for over a year [5]. Vertically, the species occupies depths from surface waters to more than 200 m, as shown by trawl catches and electronic tagging data [6,7]. It can reach a total length of around 1 m, weigh more than 12 kg, and live for up to 30 years [1,8,9]. Females typically achieve larger maximum sizes but exhibit slower growth rates than males. Growth rates are also influenced by water temperature, with Mediterranean populations generally displaying faster growth than those from the Atlantic [1,10].

Adult *D. labrax* typically spend the summer months in shallow coastal waters, where they feed mainly on small fish and crustaceans [7,9,11]. The decrease in water temperature in the winter triggers the migration of adults to deeper offshore waters, where they form spawning aggregations and release pelagic eggs [1,6]. Following hatching, larvae drift in open waters for up to several months, feeding on plankton while actively responding to environmental cues that guide them toward coastal nursery habitats such as estuaries and coastal lagoons [7,11,12]. Juveniles then settle in these sheltered areas, where they remain up to age 2 to 5, depending on habitat characteristics, before gradually expanding their range [1,9,10,13].

Despite the expansion of large-scale production of farmed *D. labrax*, wild-caught individuals remain highly valued by both commercial and recreational fisheries, often commanding prices up to three times higher than those of their farmed counterparts [14]. This high market value makes this species highly prized, with commercial landings in Europe reaching €43.8 million at first sale, while the estimated economic value of recreational fishing is approximately €356 million [14]. In the northeastern Atlantic, *D. labrax* populations are managed by the International Council for the Exploration of the Sea (ICES), which has defined four assessment units for this species: (1) West of Scotland and Ireland (Divisions 6a, 7b,j), (2) North Sea, Channel, Celtic Sea, and Irish Sea (Divisions 4–7), (3) Bay of Biscay (Divisions 8a–b), and (4) Atlantic–Iberian waters (Divisions 8c, 9a) [15]. Currently, ICES provides scientific advice for only two of these population-units: the "northern" stock (Divisions 4–7) and the "southern" stock (Divisions 8a–b) [16]. In northern Europe, *D. labrax* populations have already undergone severe declines due to overfishing, driven by both commercial and recreational sectors targeting spawning aggregations [17,18]. Although management measures such as seasonal closures and catch limits have since been implemented, recovery has remained slow [16]. In contrast, the Iberian *D. labrax* stock is

still largely unassessed and unregulated. Classified as a "data-limited stock," it has been managed under a precautionary approach since 2014 [19]. However, annual landings in ICES divisions 8c–9a have consistently exceeded the recommended limits, remaining above the advised threshold for the past decade. In 2024, landings reached 846 tonnes, more than twice the precautionary approach level of ≤382 tonnes per year [19]. Furthermore, there are no enforced seasonal closures to protect the species during its breeding period. This lack of data and proper stock management highlights the urgent need for more scientific research to better evaluate and understand the dynamics of *D. labrax* populations in the Atlantic waters of the Iberian Peninsula [19].

A critical component of this understanding involves unravelling the species' population structure, describing how individuals are organized and differentiated, shaped by factors such as genetic diversity, morphology, and spatial distribution [18,20,21]. In fish ecology, geographically isolated groups that exhibit distinct life-history or demographic traits are recognized as separate stocks, which may have unique responses to environmental variability, fishing pressure, and conservation measures [21,22]. Their stock identification and independent assessment are therefore essential to ensure sustainable exploitation and long-term population resilience [20,21]. Multiple approaches have been developed to assess the spatial isolation in fish and to identify population units. Although genetic techniques (e.g., mitochondrial DNA, nuclear markers, and single nucleotide polymorphisms [SNPs]) are widely used to define population boundaries, they are most effective when populations have experienced long-term reproductive isolation [18,21,23]. These techniques may not always be able to discriminate among different fish stocks, as even a small degree of mixing can be sufficient to homogenize genetic variation [24]. Consequently, phenotypic approaches, including body morphometrics, otolith shape and chemistry, parasite assemblages, as well as fish tagging and telemetry, can offer more recent insights into fish movements and population connectivity, providing a more accurate reflection of the current stock structure [21,25,26]. These phenotypic methods are often more cost-effective and sensitive to recent ecological differentiation that may not yet be reflected genetically [27–29]. Consequently, modern stock identification studies increasingly adopt holistic and multidisciplinary approaches that integrate multiple natural markers that provide different perspectives on the population structure, thereby enhancing the likelihood of accurately delineating different stocks [27,30,31].

Body and otolith phenotypic traits, initially assumed to be purely genetic [32], are now recognized as products of both heredity and environmental influence [21,33]. When populations become geographically isolated or exposed to distinct environmental conditions and selective pressures for enough time (e.g., water temperature and salinity or feeding regime), they may develop body and otolith characteristics that, when quantified, serve as natural tags of habitat use and population differentiation [21,27,34]. Both body morphometric and otolith shape analysis are considered effective tools for fish-stock identification and have proven successful in resolving fish-stock structure in high gene-flow systems, when environmental heterogeneity exists [27,35,36]. The combined use of both tools proved to provide a more complete view of the population structure in marine fish [27,31,37].

Several genetic studies (including microsatellites, SNPs, and genome-wide data) have consistently shown that *D. labrax* is divided into two deeply divergent lineages: an Atlantic lineage and a Mediterranean lineage, separated across the Almeria–Oran front. However, little or no clear population genetic structure along the Northeast Atlantic range was found, apart from weak signals in certain local areas. *D. labrax* in this region appears to form a single genetically connected population (metapopulation), with high gene flow and weak spatial structure [38–40]. Movements of *D. labrax* have been investigated around British waters and the Bay of Biscay using a range of complementary approaches, including genetic

analyses (microsatellites and SNP genotyping), otolith microchemistry (laser ablation), and tagging techniques (mark–recapture and electronic tagging) [7,26,38]. Genetic markers suggest long-term mixing among populations across this region, whereas phenotypic tools and tagging have revealed that many individuals display site fidelity to both summer feeding areas and winter spawning grounds [7,26]. Although *D. labrax* is generally considered a partially migratory species, some individuals exhibit residency and spawn in coastal areas [1,7,26]. Further south, along the Iberian Peninsula, genetic analyses of juvenile seabass from nursery grounds along the Portuguese coast revealed some population differentiation. An allozyme-based study identified a distinct southern population (Faro coast) with allele frequencies resembling those of Mediterranean samples, suggesting restricted gene flow between northern and southern Portuguese locations [41]. The previous studies support the use of complementary phenotypic indicators such as body morphology and otolith shape in combination with ecological knowledge to assess population structure

To address the current knowledge gap and provide important scientific advice for sustainable fisheries management, the present study investigated the population structure and habitat use of *D. labrax* in Atlantic Iberian waters by applying two complementary phenotypic approaches: (1) body geometric morphometrics using truss network analysis and (2) otolith shape contour using elliptic Fourier descriptors. By integrating both methods, this study aims to determine whether *D. labrax* individuals in the Atlantic waters Iberian Peninsula constitute a single stock, or multiple partially isolated populations. The results will provide critical insights to support ICES assessments and guide the sustainable management of this currently unassessed division.

2. Materials and Methods

2.1. Fish Sampling

Adult individuals of *D. labrax* were collected at three locations along the Atlantic coast of the Iberian Peninsula [Avilés (northern Spain), Peniche (central Portugal), and Lagos (southern Portugal)] between January and March 2025 (Figure 1). Because only adult fish were sampled and all collections occurred within a three-month window, short-term intra-annual fluctuations in body morphology and otolith shape are expected to be negligible [42]. A total of 140 individuals were captured and used for body morphometric and otolith shape and analyses: 47 from Avilés, 48 from Peniche, and 45 from Lagos (Table 1). Specimens were captured by local small-scale fishers using longlines and gillnets and purchased at public first-sale auctions, with landing sites corresponding to well-defined capture locations. This sampling strategy minimizes potential overlap among areas. Although *D. labrax* can exhibit seasonal movements, recent tagging and telemetry studies show that many individuals display strong site fidelity to summer feeding and winter spawning areas, as well as region-specific residency in coastal areas for extended periods [43,44]. These findings support the assumption that the sampling regions used in this study can be treated as relatively discrete for body and otolith shape comparisons, despite some seasonal movement. Following landing, fish were stored in ice and immediately transported to the laboratory. Total length (TL, $\pm$0.1 cm) was recorded, and each individual was photographed with anatomical landmarks indicated by pins for further geometric morphometrics analysis. Both sagittal otoliths were extracted from the skulls using forceps, cleaned of adhering tissue, left to dry, and stored in plastic tubes for later otolith shape analyses. Left and right otoliths were distinguished according to the orientation of the *sulcus acusticus* and the *rostrum* [45]. Finally, fish were carefully dissected to remove the gonads for histology processing to confirm the sex and maturity under microscope observation.

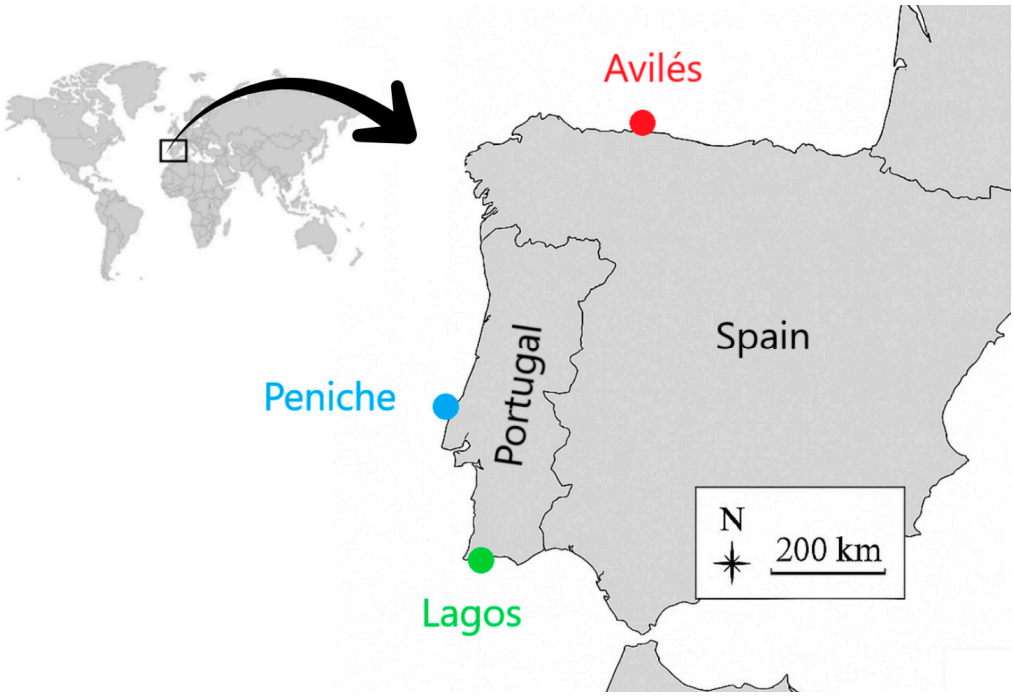

Figure 1. Location of the Iberian Peninsula in the world map (black box) and the three sampling locations (Avilés, Peniche and Lagos–coloured dots) in the Northeast Atlantic (main map) where *Dicentrarchus labrax* individuals used in this study were caught between January and March 2025.

Table 1. Location, date of collection, sample size (*n*), total length (TL) (mean ± standard error) and age (range) of *Dicentrarchus labrax* used for otolith shape and body morphometrics. Age was estimated by counting the annual growth increments in otoliths using a stereomicroscope against a dark background.

Location	Date of Collection	*n*	TL (cm)	Age (Years)
Avilés	14 January 2025	47	41.7 ± 0.3	3–5
Peniche	12 February 2025	48	44.3 ± 0.3	2–5
Lagos	25 March 2025	45	45.3 ± 0.5	2–4

2.2. Sex Determination

After dissection, gonads were carefully extracted and fixed in Bouin's solution for 24h, then stored in 70% ethanol until tissue processing. Samples were subsequently processed with a tissue processor (Diapath, Donatello series 2, Martinengo, Italy) following classical histological techniques, including dehydration in a graded ethanol series, clearing in xylene, and impregnation in paraffin. Followed by embedding in paraffin (Leica, EG1140H, Wetzlar, Germany), sectioning at 3 µm with a rotary microtome (Leica, RM2255, Wetzlar, Germany), hematoxylin-eosin staining and slide mounting [46]. Sex identification was performed by transmitted light optical microscopy (Olympus, CX41, Tokyo, Japan), coupled with a USB camera (Olympus, SC30, Tokyo, Japan) based on the morphological characteristics observed in histological sections, such as the presence of specific structures of testicular tissue (seminiferous tubules, spermatogonia, spermatocytes, spermatozoa) or ovarian tissue (oogonia, oocytes at different stages of development, follicles, theca, granulosa layer). The classification of sexual development stage was carried out according to histological criteria defined for *Danio rerio* adapted to the species under study [47]. All fish used in this study were successfully sexed and confirmed as mature individuals (Figure 2).

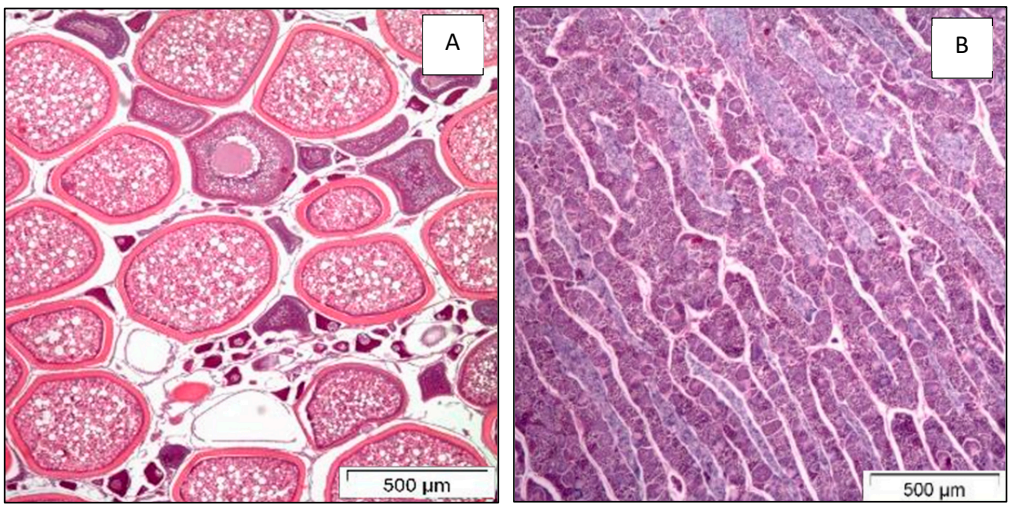

Figure 2. Representative examples of the histological classification system applied to the gonads of *Dicentrarchus labrax*, based on the defined criteria. Images were obtained by light microscopy at a total magnification of 40× using hematoxylin-eosin staining. Both specimens were caught on 14 January 2025 in Avilés. (**A**) The female (ovaries) was 43.4 cm; (**B**) The male (testis) measured 44.2 cm.

2.3. Body Geometric Morphometrics

The body morphometrics of *D. labrax* were analyzed using a Truss Network system standard protocol [48]. This method was selected for its practical, non-destructive, and sensitivity to subtle morphological variation between subpopulations [27–29]. It relies on the definition of a series of homologous landmarks along the contour of the fish's body and measures the distances between them to quantify the overall body shape. For this analysis, the left side of each fish was photographed from a fixed distance with the fins in an extended position. A precise scale (10 mm) was included in the frame, and images were captured using a Sony IMX363 high-resolution digital camera (CMOS, 12 MP sensor; image resolution: 4032 × 3024 pixels; Sony Corporation, Tokio, Japan). A total of 14 anatomic landmarks (Figure 3, Table 2) were defined in specific anatomic points, easily identifiable in all fish, determining 29 distances (Figure 3, Table 2). Landmarks were performed on the digital images using TpsUtil (ver. 1.83) and TpsDig2 (ver. 2.31). This is a user-friendly interface that allows for precise placement and recording of the X and Y coordinates of each landmark, enabling the construction of a truss network. Vertex positions were estimated from the X and Y coordinates of all specimens using the least squares method [27–29].

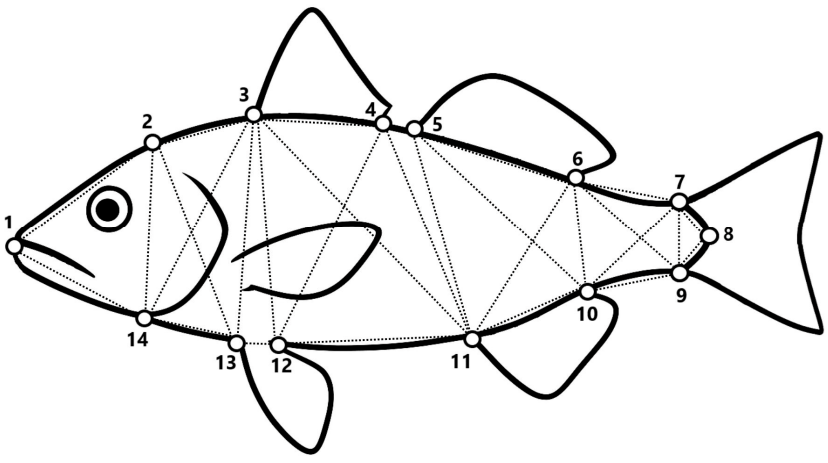

Figure 3. Location of the 14 landmarks (numbers) in the fish's left side and the corresponding morphometric distances (dashed lines). For more information see also Table 2.

Table 2. Body landmarks defined along the body contour of *Dicentrarchus labrax* and morphometric distances used for the body shape analysis. For more details, please see also Figure 3.

Body Landmarks		
Number	**Location**	
1	Anterior tip of the mouth	
2	Most posterior aspect of neurocranium	
3	Anterior insertion of the 1st (spiny) dorsal fin	
4	Posterior insertion of the 1st (spiny) dorsal fin	
5	Anterior insertion of the 2nd (soft-rayed) dorsal fin	
6	Posterior insertion of the 2nd (soft-rayed) dorsal fin	
7	Dorsal insertion of the caudal fin	
8	Posterior margin of the caudal peduncle	
9	Ventral insertion of the caudal fin	
10	Posterior insertion of the anal fin	
11	Anterior insertion of the anal fin	
12	Posterior insertion of the pelvic fin	
13	Anterior insertion of the pelvic fin	
14	Ventral insertion of the operculum	
Morphometric Distances		
Number	**Landmarks**	**Description**
D1	1 to 2	Head length
D2	1 to 14	Maxilla length
D3	2 to 3	Distance from the most posterior aspect of neurocranium to the 1st dorsal fin
D4	2 to 13	Posterior height of head
D5	2 to 14	Anterior height of head
D6	3 to 13	Anterior body height
D7	3 to 14	Distance from the posterior tip of the mouth to the anterior insertion of the 1st dorsal fin
D8	13 to 12	Length of pelvic fin
D9	13 to 14	Distance from maxilla to pelvic fin
D10	3 to 4	Length of 1st (spiny) dorsal fin
D11	3 to 11	Distance between the origin of 1st dorsal fin and the origin of anal fin
D12	3 to 12	Distance from the anterior insertion of the (spiny) dorsal fin to the posterior insertion of the pelvic fin
D13	4 to 11	Posterior body height
D14	4 to 12	Distance from the anterior insertion of the caudal fin to the anterior insertion of the 2nd dorsal fin
D15	11 to 12	Distance between pelvic fin and anal fin
D16	4 to 5	Distance between 1st and 2nd dorsal fins
D17	5 to 6	Length of 2nd dorsal fin
D18	5 to 10	Anterior diagonal height of posterior body
D19	5 to 11	Distance from the anterior insertion of the anal fin to the anterior insertion of the 2nd dorsal fin
D20	6 to 10	Anterior caudal peduncle height
D21	6 to 11	Distance from the anterior insertion of the anal fin to the posterior insertion of the 2nd dorsal fin
D22	10 to 11	Length of anal fin
D23	6 to 7	Distance between 2nd dorsal fin and caudal fin
D24	6 to 9	Anterior diagonal of caudal peduncle
D25	7 to 9	Posterior caudal peduncle height
D26	7 to 10	Posterior diagonal of caudal peduncle
D27	9 to 10	Distance between anal fin and caudal fin
D28	7 to 8	Distance between the dorsal insertion of caudal fin and the posterior end of vertebrate column
D29	8 to 9	Distance between the ventral insertion of caudal fin and the posterior end of vertebrate column

2.4. Otolith Shape Contour

The otolith shape contour was analyzed using elliptical Fourier descriptors (EFD) which quantifies the otolith outline as a closed curve and decomposes it into a set of harmonics that summarize its geometry across multiple scales and orientations [27,29,30]. This method offers a straightforward semi-automated implementation and has demonstrated high discriminatory capacity in distinguishing fish stocks [27,29,30]. Bilateral asymmetry in otolith shape is very unlike for *D. labrax*. A mixed-effects model detected no significant directional asymmetry differences between left and right otolith shape using EFD after 100 days post-hatching in *D. labrax* [49]. Consequently, all left *sagittae* were photographed, positioned with the *sulcus acusticus* facing up and the *rostrum* pointed to the left (Figure 4A). Pictures were taken under reflected light against a dark background using a Sony IMX363 high-resolution digital camera at 5× magnification (CMOS, 12 MP sensor with an image resolution of 4032 × 3024 pixels. Sony Corporation, Tokyo, Japan). The black and white contrasts to binary digital images (Figure 4B) were obtained using the free software Paint 3D (v.2024.2410.13017.0). The programme Shape v.1.3 was used to extract the otolith contour and to determine the number of EFD required to adequately describe the otolith outline [27,29,30]. The software generated 20 harmonics, each containing four coefficients (a, b, c and d), resulting in a total of 80 EFD (20 harmonics × 4 coefficients). The harmonics for each otolith were normalized to the first harmonic to ensure invariance with respect to otolith size [27,50,51]. Consequently, the first three coefficients (a1, b1 and c1) were considered invariant and have been excluded. The first 6 harmonics (excluding coefficient d6) reached 95% of the cumulative power indicating that the otolith shape contour could be summarized by 20 EFD [i.e., 6 (harmonics) × 4 (coefficients: a, b, c and d) − 3 (a1, b1, c1) − 1 (d6)]. Mean otolith outlines were quantified using standardized EFD (Figure 4C).

2.5. Statistical Analyses

Raw data were checked for normality (Shapiro–Wilk's test), variance homogeneity (Brown Forsythe's test) and equal within-group covariance matrices (inspection of discriminant function scores) [52]. For morphometric distances, the potential effects of fish size were assessed before spatial comparisons. The relationship between each distance (D) and total length (TL) was tested with One-Way Analysis of Co-variance (ANCOVA), revealing significant positive correlations ($p < 0.05$). Location was treated as a fixed factor, and TL as a covariate. The morphometric distances were corrected to eliminate any variation resulting from allometric growth. Thus, the following transformation was used:

$$TD = 10\hat{}[\log(D) - \beta\ [\log(TL) - \log(TLmean)]$$

where TD is the transformed distance, D is the original distance, β is the slope of the regression of log(D) on log(TL), TL is the total length of the individual, and TLmean is the overall mean total length for all locations [53]. The effect of sex on the variation in morphometric distances (TD) within locations was first assessed using a Two-Way Analysis of Variance (ANOVA) with location and sex as factors. Significant influence of sex for TD6, TD10, TD12 and TD14 was verified ($p < 0.05$) and therefore these distances were removed from subsequent analyses. The same analysis was applied to the elliptic Fourier descriptors (EFD); however, no significant effect of sex was detected for any descriptor ($p > 0.05$), and therefore all EFD were retained for subsequent analyses. One-Way Analysis of Variance (ANOVA) was used to explore differences in TD and EFD among locations. If significant differences were found ($p < 0.05$), this was followed by a Tukey pairwise post hoc test. Multivariate Analysis of Variance (MANOVA) was used to test for spatial differences in TD, EFD and both combined. For the MANOVA, the approximate F-ratio statistic for the

most robust test of multivariate statistics (Pillai's trace) was reported. Post hoc multivariate pairwise comparisons between regions were performed using Hotelling's T^2 test. Linear Discriminant Function Analysis (LDFA) was applied to visualize spatial differences, and the correct re-classification of individuals to their original sampling location was evaluated using a jackknifed re-classification matrix [27,30,36]. All these statistical analyses were performed using Systat (ver. 13.0), Sigmaplot (ver. 16.0) and Past (ver. 4.03). The statistical level of significance (α) was 0.05.

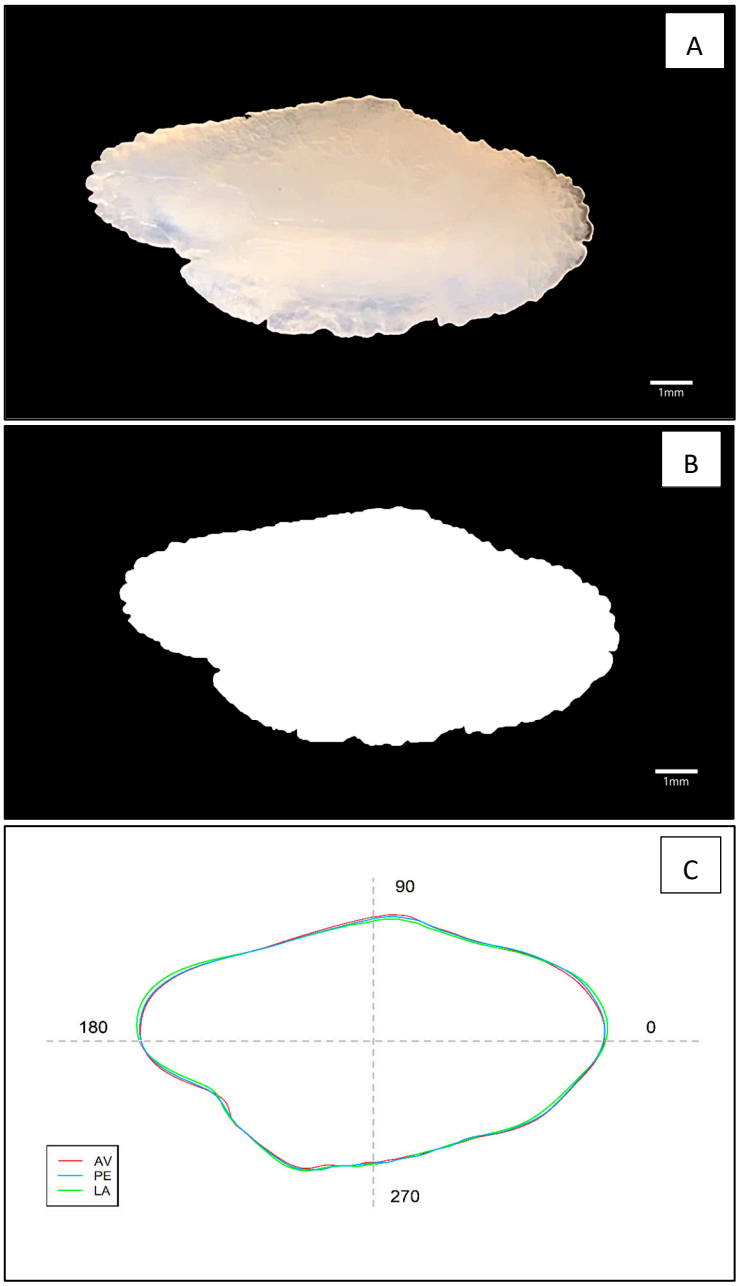

Figure 4. Left sagittal otolith of *Dicentrarchus labrax*. (**A**) original photograph; (**B**) corresponding binary digital image; (**C**) Averaged outline contour for each location. Avilés (AV: red line); Peniche (PE: blue line); Lagos (LA: green line).

3. Results

3.1. Body Geometric Morphometrics

Univariate tests showed significant differences in body morphology between at least two of the regions for 16 out of 25 distances (29 initial − 4 which sex influenced significantly)

(One-Way ANOVA followed by a Tukey test, $p < 0.05$). Two measurements (TD1 and TD3) presented significant differences among all sampling locations and three measurements differed Avilés from all other locations (TD8, TD9 and TD24) (Table 3).

Table 3. Results from the univariate statistics of the transformed body-morphometric distances and elliptical Fourier descriptors calculated for *Dicentrarchus labrax*. Values are presented as mean ± standard error. For each row, variables showing different superscript letters among locations indicate significant statistical differences (One-Way ANOVA, followed, if needed, by a post hoc pairwise Tukey test $p < 0.05$).

	Avilés	Peniche	Lagos
Transformed Distances			
TD1	9.68 ± 0.11 ^{a}	8.86 ± 0.08 ^{b}	9.23 ± 0.11 ^{c}
TD2	8.39 ± 0.11 ^{a}	8.52 ± 0.08 ^{ab}	8.82 ± 0.08 ^{b}
TD3	5.50 ± 0.07 ^{a}	6.11 ± 0.05 ^{b}	5.91 ± 0.05 ^{c}
TD4	9.56 ± 0.07 ^{a}	9.63 ± 0.06 ^{a}	9.64 ± 0.06 ^{a}
TD5	7.82 ± 0.06 ^{a}	7.54 ± 0.04 ^{b}	7.70 ± 0.05 ^{ab}
TD7	10.75 ± 0.08 ^{a}	10.50 ± 0.05 ^{b}	10.54 ± 0.06 ^{ab}
TD8	1.90 ± 0.03 ^{a}	2.20 ± 0.05 ^{b}	2.23 ± 0.04 ^{b}
TD9	4.85 ± 0.07 ^{a}	4.35 ± 0.08 ^{b}	4.47 ± 0.05 ^{b}
TD11	15.43 ± 0.10 ^{a}	15.95 ± 0.13 ^{a}	15.51 ± 0.08 ^{a}
TD13	9.41 ± 0.07 ^{a}	9.74 ± 0.09 ^{b}	9.62 ± 0.07 ^{ab}
TD15	12.37 ± 0.1 ^{a}	12.19 ± 0.22 ^{a}	11.99 ± 0.09 ^{a}
TD16	1.09 ± 0.04 ^{a}	1.08 ± 0.06 ^{a}	1.21 ± 0.06 ^{a}
TD17	6.91 ± 0.07 ^{a}	7.26 ± 0.14 ^{b}	7.22 ± 0.06 ^{ab}
TD18	10.23 ± 0.08 ^{a}	10.46 ± 0.05 ^{b}	10.30 ± 0.06 ^{ab}
TD19	8.99 ± 0.07 ^{a}	9.41 ± 0.11 ^{b}	9.21 ± 0.06 ^{ab}
TD20	5.26 ± 0.05 ^{ab}	5.51 ± 0.14 ^{a}	5.19 ± 0.04 ^{b}
TD21	7.82 ± 0.06 ^{a}	8.45 ± 0.03 ^{a}	8.10 ± 0.06 ^{a}
TD22	4.95 ± 0.05 ^{a}	5.28 ± 0.16 ^{a}	5.12 ± 0.06 ^{a}
TD23	6.66 ± 0.10 ^{a}	6.40 ± 0.09 ^{ab}	6.31 ± 0.07 ^{a}
TD24	8.19 ± 0.10 ^{a}	7.87 ± 0.06 ^{b}	7.80 ± 0.07 ^{b}
TD25	4.36 ± 0.05 ^{a}	4.27 ± 0.07 ^{a}	4.44 ± 0.04 ^{a}
TD26	7.40 ± 0.08 ^{a}	7.42 ± 0.12 ^{a}	7.37 ± 0.07 ^{a}
TD27	5.70 ± 0.07 ^{a}	5.43 ± 0.05 ^{b}	5.50 ± 0.08 ^{ab}
TD28	2.95 ± 0.03 ^{a}	3.00 ± 0.02 ^{a}	2.92 ± 0.03 ^{a}
TD29	2.95 ± 0.03 ^{a}	3.13 ± 0.04 ^{a}	3.00 ± 0.03 ^{a}
Elliptical Fourier Descriptors			
D1	0.0014 ± 0.0036 ^{a}	0.0020 ± 0.0036 ^{a}	−0.00262 ± 0.0042 ^{a}
A2	0.0019 ± 0.0039 ^{a}	0.0033 ± 0.0033 ^{a}	−0.00548 ± 0.0032 ^{a}
B2	−0.0057 ± 0.0039 ^{a}	0.0009 ± 0.00211 ^{ab}	0.0052 ± 0.0027 ^{b}
C2	−0.0052 ± 0.0020 ^{a}	−0.0007 ± 0.0022 ^{a}	0.0066 ± 0.0024 ^{b}
D2	0.0009 ± 0.0017 ^{a}	0.0008 ± 0.0015 ^{a}	−0.002 ± 0.0021 ^{a}
A3	0.0030 ± 0.0012 ^{a}	−0.0031 ± 0.0013 ^{b}	0.0003 ± 0.016 ^{a}
B3	0.0007 ± 0.001 ^{a}	0.0008 ± 0.0019 ^{a}	−0.0013 ± 0.0014 ^{a}
C3	−0.0003 ± 0.0010 ^{ab}	−0.0023 ± 0.0009 ^{a}	0.0028 ± 0.0013 ^{b}
D3	−0.0012 ± 0.0009 ^{a}	0.0010 ± 0.0012 ^{a}	0.0001 ± 0.0009 ^{a}
A4	−0.0018 ± 0.0009 ^{a}	0.0009 ± 0.0008 ^{a}	0.0009 ± 0.0010 ^{a}
B4	−0.0002 ± 0.0009 ^{a}	0.0004 ± 0.0010 ^{a}	0.0003 ± 00008 ^{a}
C4	0.010 ± 0.0007 ^{a}	0.0001 ± 0.0008 ^{a}	−0.0011 ± 0.0010 ^{a}
D4	0.0011 ± 0.0006 ^{a}	−0.0009 ± 0.0007 ^{a}	−0.0002 ± 0.0008 ^{b}
A5	0.0013 ± 0.0006 ^{a}	0.0007 ± 0.007 ^{a}	−0.0021 ± 0.0007 ^{b}
B5	−0.0001 ± 0.0008 ^{a}	−0.0002 ± 0.0006 ^{a}	0.0002 ± 0.0006 ^{a}
C5	0.0014 ± 0.0006 ^{a}	−0.0007 ± 0.0006 ^{b}	−0.0008 ± 0.0007 ^{b}
D5	0.0002 ± 0.0005 ^{a}	0.0001 ± 0.0005 ^{a}	−0.0004 ± 0.0007 ^{a}
A6	0.0006 ± 0.0006 ^{a}	−0.0004 ± 0.0006 ^{a}	−0.0002 ± 0.0005 ^{a}
B6	−0.0003 ± 0.0005 ^{a}	−0.0001 ± 0.0005 ^{a}	0.0004 ± 0.0006 ^{a}
C6	0.0004 ± 0.0004 ^{a}	−0.0007 ± 0.0006 ^{a}	0.0003 ± 0.0006 ^{a}

MANOVA statistical tests performed on the TD presented significant differences among the sampling locations (Pillai's Trace: F-ratio = 4.864, $p < 0.05$).

The plot obtained in the LDFA showed a significant overlap of individuals from all locations (Figure 5A). The jackknife matrix indicated an overall modest reclassification score of 68%. Samples from Lagos exhibited the lowest score with 56% reclassification, whereas Peniche and Avilés displayed highest accuracies with 71% and 77%, respectively (Table 4).

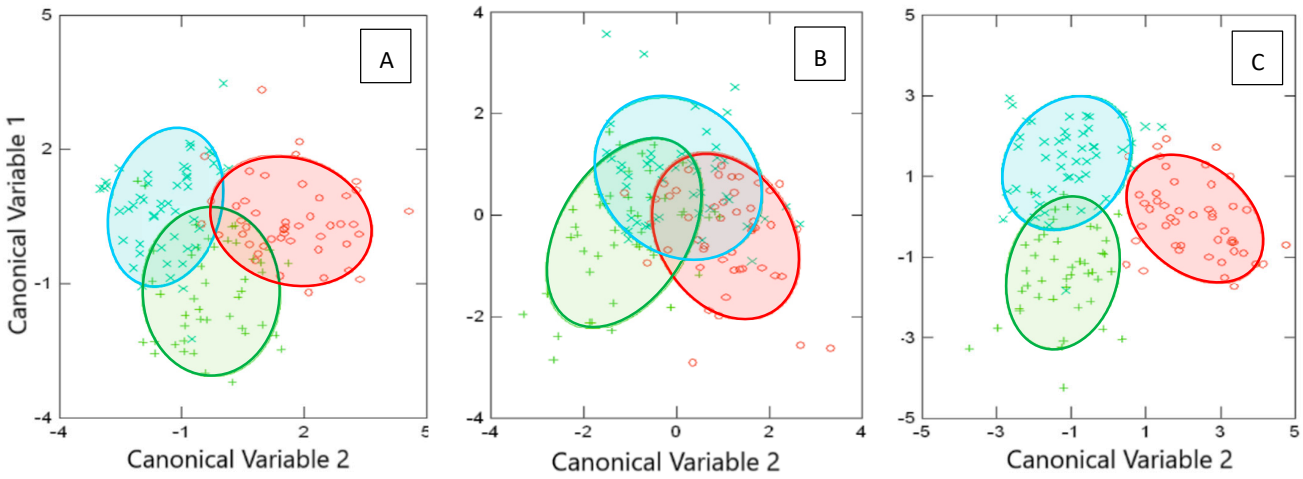

Figure 5. Linear Discriminant Function Analysis (LDFA) plots displaying spatial differences for (**A**) truss network (Transformed Distances), (**B**) otolith shape (Elliptical Fourier Descriptors) and (**C**) both approaches combined from *Dicentrarchus labrax*. Ellipses represent 95% confidence intervals around the data, and each data point represents an individual fish. Locations: Avilés (red circles), Peniche (blue crosses) and Lagos (green plus signs).

Table 4. Jack-knifed cross validation re-classification matrix following a linear discriminant function analysis based on body truss network (Transformed Distances, TD), otolith shape contour (Elliptical Fourier Descriptors, EFD), and the combination of both approaches (TD + EFD) for *Dicentrarchus labrax* individuals

Original Location				**Predicted Location**
TD	**Avilés**	**Peniche**	**Lagos**	**%Correct**
Avilés	36	4	7	77
Peniche	3	34	11	71
Lagos	11	9	25	56
Total	50	47	43	68
Original Location				**Predicted Location**
EFD	**Avilés**	**Peniche**	**Lagos**	**%Correct**
Avilés	29	14	4	62
Peniche	13	17	18	35
Lagos	5	14	26	58
Total	47	45	48	51
Original Location				**Predicted Location**
TD + EFD	**Avilés**	**Peniche**	**Lagos**	**%Correct**
Avilés	34	9	4	72
Peniche	6	28	14	58
Lagos	5	11	29	64
Total	45	48	47	65

3.2. Otolith Shape Contour

Univariate tests (One-Way ANOVAs, $p < 0.05$) showed significant differences in otolith shape among locations for 7 EFD (b2, c2, a3, c3, a5 and c5). Two EFD differed Lagos from all other locations (c2 and a5); no measurements differentiated Peniche or Lagos from the other locations (Tukey tests, $p < 0.05$) (Table 3). MANOVA statistical tests performed on the EFD presented significant differences among the sampling locations (Pillai's Trace: F-ratio = 2.951, $p < 0.05$). The plot obtained in the LDFA showed a significant overlap of individuals from all locations (Figure 5B). The jackknife matrix indicated an overall score of 51% reclassification. Samples from Lagos exhibited the lowest reclassification score with 35%, whereas Peniche and Avilés displayed better accuracies with 58% and 62%, respectively (Table 4). The mean otolith contour image (Figure 4C) displays the averaged otolith shapes for each location. Avilés' contour is slightly narrower along the horizontal axis (0–180°) and taller along the vertical axis (90–270°) compared to Lagos', which is wider left–right and shorter vertically.

3.3. Combination of Both Approaches

The combination of both TD and EFD resulted in an overall reallocation of 65% (Table 4). The best reclassification was for Avilés with 72%, while the lowest was obtained for Peniche (58%). The LDFA plot shows no overlap between Avilés and the other locations (Figure 5C) despite the decrease in correct reallocation (Table 4). MANOVA statistical test, followed by Hotelling's T^2 ($p < 0.05$) performed on the combination of data presented significant differences between all locations (Pillai's Trace: F ratio = 3.995, $p < 0.001$).

4. Discussion

The phenotypic indicators used in this study, namely body morphometrics and otolith shape, are cost-effective, relatively easy to observe, and require minimal equipment, while providing objective and reproducible data for detecting population differentiation [27,29,37]. Body truss network analysis captures overall body shape variation and enables quantitative comparisons among populations; however, body morphometric traits may be influenced by phenotypic plasticity and environmental conditions, potentially reflecting morphological differences not solely driven by genetic differentiation [27,35,54]. Otolith shape analysis allows fine-scale discrimination among populations and is relatively stable over an individual's lifetime, although otolith morphology can also be affected by environmental factors experienced during growth [33,36,55]. Both methods require standardized measurement protocols, adequate sample sizes, specialized imaging, and complex statistical analyses. Despite these limitations, the combined use of body morphometric and otolith shape contour analyses provides a complementary and robust framework that integrates external and internal phenotypic signals, enhancing the reliability of population structure assessment and making these approaches suitable for large-scale or preliminary investigations [27,31,37].

Previous studies have investigated *Dicentrarchus labrax* population structure in the northern ICES divisions and in the Bay of Biscay using tagging, genetic and otolith elemental analyses [7,26,43]. These studies showed that it is a highly mobile species capable of long-distance migrations, yet individuals often display strong site fidelity to winter spawning and summer feeding areas, with evidence also suggesting natal homing [7,26]. Tagging and recapture studies point to the existence of two distinct stocks: one in the Bay of Biscay and another encompassing the English Channel and the Celtic Sea around the UK coasts [7,26,43,56–58]. Genetic studies of *D. labrax* in the Northeast Atlantic have consistently reported very low levels of genetic differentiation among sampling locations, indicating that populations within this region form a largely genetically connected metapop-

ulation, with only subtle signals of regional differentiation [38–41,56]. Nevertheless, minor local differences and introgression gradients have been detected, highlighting that neutral genetic structure alone may not fully capture demographic or phenotypic variation. This low level of genetic spatial differentiation therefore supports the use of complementary, heterogeneous phenotypic indicators to investigate population structure. Indeed, genetic markers primarily reflect evolutionary and long-term gene flow, integrating population connectivity over multiple generations and often showing limited sensitivity to recent or short-term demographic processes. In contrast, phenotypic indicators can respond to environmental conditions and developmental processes within an individual's lifetime, thereby capturing more recent or contemporary population structuring [21,22]. As noted above, the Iberian divisions (8c, 9a), which are generally assumed to represent a single stock, remain largely unassessed [19].

The body shape analyses found differences in fish collected from different locations. It was verified that fish from Avilés exhibited a longer and taller head, contrary to Peniche's fish that had the smallest and shortest head (TD1 and TD5, respectively) (Table 3). Interestingly, Avilés' fish, despite a larger head, had the shortest maxilla, whereas Lagos fish had the longest (TD2) (Table 3). These differences could reflect local prey availability, as head morphology is often linked to feeding strategies [27,59,60]. Similar ecological-driven morphological variation has been observed in other species like Sparids [59] and pelagic fish such as mackerel and the blue jack mackerel [27,60]. Upwelling regimes differ markedly along the Atlantic Iberian coast, particularly between the Cantabrian Sea, the western Portuguese coast, and the Gulf of Cádiz, leading to regional differences in food availability and prey composition [61,62]. Such environmental contrasts provide a plausible ecological explanation for the head and mouth morphological divergence observed in the present study. Fish from Aviles had narrower second dorsal fins, and a shorter distance to the anal fin (TD13, TD17, TD18, and TD19), whereas Peniche fish had wider second dorsal fins (TD17) and a taller body (TD13, TD18 and TD19) (Table 3). Caudal traits also differed, with Avilés fish having longer tails (TD23, TD24, and TD27) (Table 3). Differences associated with fins and tail size are often associated with habitat hydrodynamics, fish with a streamlined morphology and deeper caudal peduncles exhibit enhanced capability to counter hydrodynamic resistance within fast-flowing water [63–66]. Contrary to the south of the Iberian Peninsula, the Cantabrian Sea, is influenced by strong tidal and wind-driven currents [67–69], possibly selecting for fast, efficient swimmers with deep caudal peduncles. Despite the overall percentage of correct reclassification being relatively low (51%) (Table 4) and some overlap of the individuals of each location in the LDFA graph (Figure 5A), the MANOVA revealed significant differences among all locations (Hotelling's T^2, $p < 0.05$). Fish from Avilés and Lagos showed the highest level of separation, as only a few individuals were misclassified between these two locations in the jackknife reclassification matrix (Table 4).

Otolith shape undergoes clear modifications during ontogeny, with the specific pattern of change strongly influenced by environmental conditions [27,51,70]. Factors such as habitat use, food availability, and temperature can affect otolith morphology beyond simple size differences [51,70,71]. Studies have shown that somatic growth rates are closely linked to otolith shape: faster-growing fish (i.e., greater length at age) tend to develop more elongated and narrow otoliths with pronounced *rostrum* and *postrostrum*, whereas slower-growing individuals display shorter, wider shapes [51,70,71]. Fish from colder waters (Avilés ~15 °C) are expected to grow slower and therefore develop more elongated, narrow otoliths, while individuals from Lagos (~19 °C) growing faster and consequently having shorter, wider otoliths, with fish from Peniche (~16 °C) displaying intermediate characteristics (mean annual sea surface water temperatures obtained from [72]). This

theoretical growth rate difference was represented in the mean otolith shape (Figure 4C). This suggests that fish were exposed to environmental conditions for sufficient time for these variables to be reflected in their growth rate and consequently in the otolith phenotype. Despite MANOVA indicating differences between otolith shapes of all locations (Hotelling's T^2, $p < 0.05$), the variation in otolith morphology across locations was relatively minor (Figure 4C) showing spatial differences in 7 out of the 20 analyzed EFD (Table 3) and high overlap in the LDFA graph (Figure 5B). This indicates some degree of connectivity among populations, which may act to homogenize otolith shape [27,37,71]. Similar studies along the Portuguese coast in both pelagic and demersal fish have also reported minor otolith shape variation across locations [27,30,36]. Studies along the Iberian and Northeast Atlantic coasts generally interpret otolith-shape differences among regions as the result of environmentally driven phenotypic plasticity rather than neutral genetic divergence. Spatial variation in temperature, upwelling intensity, productivity, and prey availability influences growth rates and metabolic processes during early life and juvenile stages, which are known to affect otolith accretion and shape [73–75]. Consequently, otolith morphology can retain a regional signature reflecting local growth and feeding conditions, even in species with high dispersal potential and weak genetic structure, consistent with the patterns observed in the present study.

Combining body morphometrics and otolith shape analyses, the LDFA plot showed a better visual isolation of fish from Avilés (Figure 5C). These results indicate a greater isolation between fish from the north and from the south since there was very low reallocation of Aviles to Lagos and vice versa (Table 4) with Peniche acting as an intermediate population. Despite this, the overall reclassification accuracy slightly decreased (Table 4). In fact, for Peniche and Avilés, the highest reclassification success was achieved using body shape alone (71% and 77%, respectively) whereas otolith shape gave the lowest scores (35% and 62%) (Table 4). Lagos was the only location where the combined approach enhanced accuracy (64%) relative to individual methods (Table 4). The absence of a significant improvement may indicate that, in Iberian fish samples, environmental and genetic variation could be more reflected in external body morphology than in otolith shape contour. Similar results were also observed in other marine fish such as *Trachurus picturatus* and *Scomber colias*, where body morphometrics showed greater discrimination than otolith shape [27,31]. Several studies on marine fishes have shown that phenotypic markers such as body morphometrics and otolith shape can reveal spatial structure not detected by neutral genetic markers, particularly when gene flow is high or when genetic sampling uses markers with limited resolution: direct comparison of microsatellite results and body-shape landmarks in *Altolamprologus compressiceps* revealed that morphological differentiation was stronger or more spatially structured than neutral genetic markers [76]; otolith-shape analyses have identified potential stock units for *Dentex dentex* while microsatellite analyses reported little or no differentiation [73]; and otolith the analysis and body morphometrics have shown the presence of, at least, three different population-units of *Trachurus picturatus* in the NE Atlantic Ocean when preliminary MtDNA markers indicated the absence of genetic structure among populations [36,54,60]. Otolith morphology and body shape integrate ontogenetic and environmental history (temperature, growth rates, salinity) and therefore may reflect recent or ecologically driven divergence, whereas traditional neutral genetic markers typically record longer-term connectivity [24]. This complementarity means phenotypic methods are especially useful to detect ecologically meaningful population structure or recent isolation, however results must be interpreted with caution because otolith and body shape are influenced by age, size, year-class and local environment; temporal replication and controlling for covariates are therefore recommended.

5. Conclusions

Effective population management and monitoring are essential to ensure adequate management frameworks to guide decision-making for environmentally and socio- economically sustainable *D. labrax* fisheries. Currently, catches of the European seabass in Iberian Peninsula water greatly exceed ICES advice. It is considered a data-limited species, lacks protective measures during the breeding season when it is particularly vulnerable to fisheries targeting spawning aggregations, and there is no stock assessment or management measures other than a minimum legal landing size of 36 cm TL and minimum mesh sizes for nets. This study, integrating geometric morphometrics and otolith shape analyses, supports ICES's designation of a single but not entirely homogeneous fish stock across the Iberian divisions (8c, 9a), with some regional differentiation likely driven by environmental and ecological factors. Although year-class effects cannot be entirely excluded, the consistency of regional discrimination across phenotypic markers supports the interpretation of environmentally mediated population structuring. To refine this assessment, future research should incorporate complementary approaches for better monitoring, such as genetic analyses, tagging and telemetry (acoustic or RFID tags), otolith chemistry, and parasite assemblages, considering a systematic sampling and collection of data over time.

Author Contributions: R.G.K.; conceptualization, methodology, formal analysis, investigation, writing—original draft, funding acquisition. R.M.S.: methodology, writing—review and editing. A.F.R.: methodology, writing—review and editing. J.S.C.: writing—review and editing, supervision. R.C.S.: methodology, writing—review and editing. E.R.: methodology, formal analysis, resources, writing—review and editing. K.E.: resources, writing—review and editing, supervision, funding acquisition. A.T.C.: conceptualization, methodology, formal analysis, investigation, resources, writing—review and editing, supervision, funding acquisition. All authors have read and agreed to the published version of the manuscript.

Funding: Rafael Gaio Kulzer received financial support from Fundação Amadeu Dias under the BYTplus program of CIIMAR 2024/2025. João Soares Carrola was supported by FCT–Portuguese Foundation for Science and Technology under the projects UID/04033/2025: Centre for the Research and Technology of Agro-Environmental and Biological Sciences and LA/P/0126/2020 (https://doi.org/10.54499/LA/P/0126/2020). Karim Erzini was supported by FCT–Portuguese Foundation for Science and Technology through contracts UID/04326/2025, UID/PRR/04326/2025 and LA/P/0101/2020 (https://doi.org/10.54499/LA/P/0101/2020). Alberto Teodorico Correia was funded by national funds through FCT—Fundação para a Ciência e a Tecnologia, I.P., and by the European Commission's Recovery and Resilience Facility, within the scope of UID/04423/2025 (https://doi.org/10.54499/UID/04423/2025), UID/PRR/04423/2025 (https://doi.org/10.54499/UID/PRR/04423/2025), and LA/P/0101/2020 (https://doi.org/10.54499/LA/P/0101/2020).

Institutional Review Board Statement: This work does not involves experimentation with live animals. Individuals (fish) were acquired in legal fish auctions markets. No national or European ethical committee is needed. We are dealing with human fishery products.

Data Availability Statement: The data presented in this study are available on request from the corresponding author.

Acknowledgments: The authors would like to thank Ángel Muñoz (Rula de Avilés), Fábio Raimundo (Docapesca) and Nuno Carrada (Docapesca) for the assistance in the fish acquisition from artisanal fishermen.

Conflicts of Interest: The authors declare no conflicts of interest.

Abbreviations

The following abbreviations are used in this manuscript:

ANCOVA	One-way Analysis of Covariance
ANOVA	One-way Analysis of Variance
D	Distance
DNA	Deoxyribonucleic Acid
EFD	Elliptical Fourier Descriptor
ICES	International Council for the Exploration of the Sea
LDFA	Linear Discriminant Function Analysis
MANOVA	Multivariate Analysis of Variance
MP	Megapixels
N	Sample Size
RFID	Radio-Frequency Identification
SNP	Single Nucleotide Polymorphism
TL	Total Length
TD	Transformed Distance
UK	United Kingdom

References

1. López, R.; De Pontual, H.; Bertignac, M.; Mahévas, S. What can exploratory modelling tell us about the ecobiology of European sea bass (*Dicentrarchus labrax*): A comprehensive overview. *Aquat. Living Resour.* **2015**, *28*, 61–79. [CrossRef]
2. Bagdonas, K.; Nika, N.; Bristow, G.; Jankauskiene, R.; Salyte, A.; Kontautas, A. First record of *Dicentrarchus labrax* (Linnaeus, 1758) from the southeastern Baltic Sea (Lithuania). *J. Appl. Ichthyol.* **2011**, *27*, 1390–1391. [CrossRef]
3. Quéré, N.; Desmarais, E.; Tsigenopoulos, C.S.; Belkhir, K.; Bonhomme, F.; Guinand, B. Gene flow at major transitional areas in sea bass (*Dicentrarchus labrax*) and the possible emergence of a hybrid swarm. *Ecol. Evol.* **2012**, *2*, 3061–3078. [CrossRef] [PubMed]
4. Almeida, R.; Tanner, S.E.; Mateus, C.S.; Ribeiro, F.; Quintella, B.R. Not so much a sea bass: Divergent European Sea bass (*Dicentrarchus labrax* L.) freshwater incursions. *J. Fish Biol.* **2024**, *104*, 1241–1246. [CrossRef]
5. Antunes, C.; Antunes, C.M.; Fernandes, M.; Dias, E. Prolonged use of freshwater habitats by the European sea bass revealed by otolith chemical analysis. *J. Fish Biol.* **2025**, *107*, 1201–1212. [CrossRef]
6. Froese, R.; Zeller, D.; Kleisner, K.; Pauly, D. What catch data can tell us about the status of global fisheries. *Mar. Biol.* **2012**, *159*, 1283–1292. [CrossRef]
7. De Pontual, H.; Lalire, M.; Fablet, R.; Laspougeas, C.; Garren, F.; Martin, S.; Drogou, M.; Woillez, M. New insights into behavioural ecology of European seabass off the West Coast of France: Implications at local and population scales. *ICES J. Mar. Sci.* **2019**, *76*, 501–515. [CrossRef]
8. Bagni, M. *Dicentrarchus labrax*. In *Cultured Aquatic Species Fact Sheets*; Crespi, V., New, M., Eds.; FAO: Rome, Italy, 2009.
9. Vázquez, F.J.S.; Munoz-Cueto, J.A. *Biology of European Sea Bass*; CRC Press: Boca Raton, FL, USA, 2014. [CrossRef]
10. Pickett, G.D.; Pawson, M.G. *Sea Bass: Biology, Exploitation and Conservation*; Chapman & Hall: London, UK, 1994; Volume 12. [CrossRef]
11. Spitz, J.; Chouvelon, T.; Cardinaud, M.; Kostecki, C.; Lorance, P. Prey preferences of adult sea bass *Dicentrarchus labrax* in the northeastern Atlantic: Implications for bycatch of common dolphin *Delphinus delphis*. *ICES J. Mar. Sci.* **2013**, *70*, 452–461. [CrossRef]
12. Leis, J.M.; Balma, P.; Ricoux, R.; Galzin, R. Ontogeny of swimming ability in the European Sea Bass, *Dicentrarchus labrax* (L.) (Teleostei: Moronidae). *Mar. Biol. Res.* **2012**, *8*, 265–272. [CrossRef]
13. Dawson, J.; Lincoln, H.; Sturrock, A.M.; Martinho, F.; McCarthy, I.D. Recruitment of European sea bass (*Dicentrarchus labrax*) in northerly UK estuaries indicates a mismatch between spawning and fisheries closure periods. *J. Fish Biol.* **2024**, *105*, 564–576. [CrossRef]
14. EUMOFA. Commercial and Recreational Fisheries for Wild Seabass in the Atlantic. In *Economic and Market Study*; Office of the European Union: Luxembourg, 2021. [CrossRef]
15. ICES. Report of the Working Group on Assessment of New MoU Species (WGNEW), 5–9 March 2012. In *ICES Expert Group Reports (Until 2018)*; ICES: Copenhagen, Denmark, 2012. [CrossRef]
16. ICES. ICES Advice 2025. In *ICES Advice*; ICES: Copenhagen, Denmark, 2025. [CrossRef]
17. Grilli, G.; Curtis, J.; Hynes, S.; O'Reilly, P. Anglers' views on stock conservation: Sea bass angling in Ireland. *Mar. Policy* **2019**, *99*, 34–41. [CrossRef]

18. ICES. Stock Identification Methods Working Group (SIMWG). In *ICES Scientific Reports*; Report; ICES: Copenhagen, Denmark, 2021. [CrossRef]
19. ICES. Sea bass (*Dicentrarchus labrax*) in divisions 8.c and 9.a (southern Bay of Biscay and Atlantic Iberian waters). In *ICES Advice: Recurrent Advice*; ICES: Copenhagen, Denmark, 2025. [CrossRef]
20. Kerr, L.A.; Hintzen, N.T.; Cadrin, S.X.; Clausen, L.W.; Dickey-Collas, M.; Goethel, D.R.; Hatfield, E.M.C.; Kritzer, J.P.; Nash, R.D.M. Lessons learned from practical approaches to reconcile mismatches between biological population structure and stock units of marine fish. *ICES J. Mar. Sci.* **2017**, *74*, 1708–1722. [CrossRef]
21. Cadrin, S.X. Defining spatial structure for fishery stock assessment. *Fish. Res.* **2020**, *221*, 105397. [CrossRef]
22. Sarakinis, K.G.; Reis-Santos, P.; Ye, Q.; Earl, J.; Gillanders, B.M. Combining natural markers to investigate fish population structure and connectivity. *Estuar. Coast. Shelf Sci.* **2024**, *308*, 108920. [CrossRef]
23. da Fonseca, R.R.; Campos, P.F.; Rey-Iglesia, A.; Barroso, G.V.; Bergeron, L.A.; Nande, M.; Tuya, F.; Abidli, S.; Pérez, M.; Riveiro, I.; et al. Population Genomics Reveals the Underlying Structure of the Small Pelagic European Sardine and Suggests Low Connectivity within Macaronesia. *Genes* **2024**, *15*, 170. [CrossRef]
24. Andersson, L.; Bekkevold, D.; Berg, F.; Farrell, E.D.; Felkel, S.; Ferreira, M.S.; Fuentes-Pardo, A.P.; Goodall, J.; Pettersson, M. How Fish Population Genomics Can Promote Sustainable Fisheries: A Road Map. *Annu. Rev. Anim. Biosci.* **2024**, *12*, 1–20. [CrossRef] [PubMed]
25. Elsdon, T.; Wells, B.; Campana, S.; Gillanders, B.; Jones, C.; Limburg, K.; Secor, D.; Thorrold, S.; Walther, B. Otolith chemistry to describe movements and life-history parameters of fishes: Hypotheses, assumptions, limitations and inferences. *Oceanogr. Mar. Biol. Annu. Rev.* **2008**, *46*, 297–330. [CrossRef]
26. Le Luherne, E.; Daverat, F.; Woillez, M.; Pécheyran, C.; de Pontual, H. Coupling natural and electronic tags to explore spawning site fidelity and natal homing in northeast Atlantic European seabass. *Estuar. Coast. Shelf Sci.* **2022**, *278*, 108118. [CrossRef]
27. Muniz, A.A.; Moura, A.; Triay-Portella, R.; Moreira, C.; Santos, P.T.; Correia, A.T. Population structure of the chub mackerel (*Scomber colias*) in the North-east Atlantic inferred from otolith shape and body morphometrics. *Mar. Freshw. Res.* **2021**, *72*, 341–352. [CrossRef]
28. Ferreira, I.; Schroeder, R.; Mugerza, E.; Oyarzabal, I.; McCarthy, I.D.; Correia, A.T. *Chelidonichthys lucerna* (Linnaeus, 1758) Population Structure in the Northeast Atlantic Inferred from Landmark-Based Body Morphometry. *Biology* **2024**, *13*, 17. [CrossRef]
29. Freitas, F.L.; Pereira, N.S.; Pinheiro, P.B.; Schroeder, R.; Correia, A.T. Assessing the population structure of *Plagioscion squamosissimus* (Teleostei, Perciformes, Sciaenidae) from the São Francisco River, Bahia, Brazil, using body morphology and otolith shape signatures. *J. Fish Biol.* **2025**, *in press*. [CrossRef] [PubMed]
30. Ferreira, I.; Santos, D.; Moreira, C.; Feijó, D.; Rocha, A.; Correia, A.T. Population structure of *Chelidonichthys lucerna* in Portugal mainland using otolith shape and elemental signatures. *Mar. Biol. Res.* **2019**, *15*, 500–512. [CrossRef]
31. Vasconcelos, J.; Cirera, M.; Vieira, A.R.; Otero-Ferrer, J.L.; Tuset, V.M. Application of shape analysis for the identification of pelagic fish stocks (*Trachurus trachurus*): Body and otolith shape using geometric morphometrics and wavelet functions. *Hydrobiologia* **2025**, *852*, 2847–2869. [CrossRef]
32. McQuinn, I.H. Metapopulations and the Atlantic herring. *Rev. Fish Biol. Fish.* **1997**, *7*, 297–329. [CrossRef]
33. Tuset, V.M.; Lozano, I.J.; González, J.A.; Pertusa, J.F.; García-Díaz, M.M. Shape indices to identify regional differences in otolith morphology of comber, *Serranus cabrilla* (L., 1758). *J. Appl. Ichthyol.* **2003**, *19*, 88–93. [CrossRef]
34. Heimbrand, Y.; Limburg, K.; Hüssy, K.; Næraa, T.; Casini, M. Cod otoliths document accelerating climate impacts in the Baltic Sea. *Sci. Rep.* **2024**, *14*, 16750. [CrossRef] [PubMed]
35. Hoff, N.T.; Dias, J.F.; Zani-Teixeira, M.L.; Soeth, M.; Correia, A.T. Population structure of the bigtooth corvina *Isopisthus parvipinnis* from the Southwest Atlantic Ocean as determined by whole-body morphology. *Reg. Stud. Mar. Sci.* **2020**, *39*, 101379. [CrossRef]
36. Moreira, C.; Froufe, E.; Vaz-Pires, P.; Correia, A.T. Otolith shape analysis as a tool to infer the population structure of the blue jack mackerel, *Trachurus picturatus*, in the NE Atlantic. *Fish. Res.* **2019**, *209*, 40–48. [CrossRef]
37. Schroeder, R.; Schwingel, P.R.; Correia, A.T. Population structure of the Brazilian sardine (*Sardinella brasiliensis*) in the South-West Atlantic inferred from body morphology and otolith shape signatures. *Hydrobiologia* **2022**, *849*, 1367–1381. [CrossRef]
38. Souche, E.L.; Hellemans, B.; Babbucci, M.; Macaoidh, E.; Guinand, B.; Bargelloni, L.; Chistiakov, D.A.; Patarnello, T.; Bonhomme, F.; Martinsohn, J.T.; et al. Range-wide population structure of European sea bass *Dicentrarchus labrax*. *Biol. J. Linn. Soc.* **2015**, *116*, 86–105. [CrossRef]
39. Robinet, T.; Roussel, V.; Cheze, K.; Gagnaire, P.A. Spatial gradients of introgressed ancestry reveal cryptic connectivity patterns in a high gene flow marine fish. *Mol. Ecol.* **2020**, *20*, 3857–3871. [CrossRef]
40. Taylor, M.I.; Lamb, P.D.; Coscia, I.; Murray, D.S.; Brown, M.; Cameron, T.C.; Davison, P.I.; Freeman, H.A.; Georgiou, K.; Grati, F.; et al. High-density SNP panel provides little evidence for population structure in European sea bass (*Dicentrarchus labrax*) in waters surrounding the UK. *ICES J. Mar. Sci.* **2025**, *82*, fsaf064. [CrossRef]
41. Castilho, R.; McAndrew, B.J. Population structure of seabass in Portugal: Evidence from allozymes. *J. Fish Biol.* **1998**, *53*, 1038–1049. [CrossRef]

42. Jónsdóttir, I.G.; Campana, S.E.; Marteinsdóttir, G. Otolith shape and temporal stability of spawning groups of Icelandic cod (*Gadus morhua* L.). *ICES J. Mar. Sci.* **2006**, *63*, 1501–1512. [CrossRef]
43. de Pontual, H.; Heerah, K.; Goossens, J.; Garren, F.; Martin, S.; Le Ru, L.; Le Roy, D.; Woillez, M.; Edwards, J.E.; De Putter, G.; et al. Seasonal migration, site fidelity, and population structure of European seabass (*Dicentrarchus labrax*). *ICES J. Mar. Sci.* **2023**, *80*, 1606–1618. [CrossRef]
44. Goossens, J.; Woillez, M.; Wright, S.; Edwards, J.E.; De Putter, G.; Torreele, E.; Verhelst, P.; Sheehan, E.; Moens, T.; Reubens, J. Elucidating the migrations of European seabass from the southern north sea using mark-recapture data, acoustic telemetry and data storage tags. *Sci. Rep.* **2024**, *14*, 13180. [CrossRef] [PubMed]
45. Secor, D.H.; Dean, J.M.; Laban, E.H. Otolith removal and preparation for microstructural examination. In *Otolith Microstructure Examination and Analysis*; Stevenson, D.K., Campana, S.E., Eds.; Canadian Special Publication of Fisheries and Aquatic Sciences: Ottawa, ON, Canada, 1992; Volume 117, pp. 19–57.
46. Suvarna, S.K.; Layton, C.; Bancroft, J.D. *Bancroft's Theory and Practice of Histological Techniques*, 8th ed.; Elsevier: Amsterdam, The Netherlands, 2019. [CrossRef]
47. OECD. *Guidance Document on the Diagnosis of Endocrine-Related Histopathology in Fish Gonads*; OECD Publishing: Paris, France, 2010. [CrossRef]
48. Strauss, R.E.; Bookstein, F.L. The Truss: Body Form Reconstructions in Morphometrics. *Syst. Biol.* **1982**, *31*, 113–135. [CrossRef]
49. Mahé, K.; Clota, F.; Blanc, M.O.; Defruit, G.B.; Chatain, B.; de Pontual, H.; Amara, R.; Ernande, B. Otolith morphogenesis during the early life stages of fish is temperature-dependent: Validation by experimental approach applied to European seabass (*Dicentrarchus labrax*). *J. Fish. Biol.* **2024**, *104*, 2032–2043. [CrossRef] [PubMed]
50. Rodgveller, C.J.; Hutchinson, C.E.; Harris, J.P.; Vulstek, S.C.; Guthrie, C.M. Otolith shape variability and associated body growth differences in giant grenadier, *Albatrossia pectoralis*. *PLoS ONE* **2017**, *12*, e0180020. [CrossRef]
51. Campana, S.E.; Casselman, J.M. Stock discrimination using otolith shape analysis. *Can. J. Fish. Aquat. Sci.* **1993**, *50*, 1062–1083. [CrossRef]
52. Quinn, G.P.; Keough, M.J. *Experimental Design and Data Analysis for Biologists*; Cambridge University Press: Cambridge, UK, 2002. [CrossRef]
53. Reist, J. An empirical evaluation of several univariate methods that adjust for size variation in morphometric data. *Can. J. Zool.* **2011**, *63*, 1429–1439. [CrossRef]
54. Moreira, C.; Froufe, E.; Vaz-Pires, P.; Triay-Portella, R.; Correia, A.T. Landmark based geometric morphometrics analysis of body shape variation among populations of the blue jack mackerel, *Trachurus picturatus*, from the North-East Atlantic. *J. Sea Res.* **2020**, *163*, 101926. [CrossRef]
55. Federica, S.; Silvio, K.; Umberto, S.; Andrea, D.G.; Massimiliano, S. Population-level shape variation and otolith asymmetry in *Diplodus annularis*. *Sci. Rep.* **2025**, *15*, 87096. [CrossRef]
56. Fritsch, M.; Morizur, Y.; Lambert, E.; Bonhomme, F.; Guinand, B. Assessment of sea bass (*Dicentrarchus labrax*, L.) stock delimitation in the Bay of Biscay and the English Channel based on mark-recapture and genetic data. *Fish. Res.* **2007**, *83*, 123–132. [CrossRef]
57. Doyle, T.K.; Haberlin, D.; Clohessy, J.; Bennison, A.; Jessopp, M. Localised residency and inter-annual fidelity to coastal foraging areas may place sea bass at risk to local depletion. *Sci. Rep.* **2017**, *7*, 45841. [CrossRef] [PubMed]
58. O'Neill, R.; Ó Maoiléidigh, N.; McGinnity, P.; Bond, N.; Culloty, S. The novel use of pop-off satellite tags (PSATs) to investigate the migratory behaviour of European sea bass *Dicentrarchus labrax*. *J. Fish Biol.* **2018**, *92*, 1404–1421. [CrossRef] [PubMed]
59. Palma, J.; Andrade, J.P. Morphological study of *Diplodus sargus*, *Diplodus puntazzo*, and *Lithognathus mormyrus* (Sparidae) in the Eastern Atlantic and Mediterranean Sea. *Fish. Res.* **2002**, *57*, 1–8. [CrossRef]
60. Moreira, C.; Correia, A.T.; Vaz-Pires, P.; Froufe, E. Genetic diversity and population structure of the blue jack mackerel *Trachurus picturatus* across its western distribution. *J. Fish Biol.* **2019**, *94*, 725–731. [CrossRef]
61. Alvarez, I.; Gomez-Gesteira, M.; de Castro, M.; Lorenzo, M.N.; Crespo, A.J.C.; Dias, J.M. Comparative analysis of upwelling influence between the western and northern coast of the Iberian Peninsula. *Cont. Shelf Res.* **2011**, *31*, 388–399. [CrossRef]
62. del Rosario, J.J.A.; Gómez, E.B.; Pérez, J.M.V.; Rey, F.M.; Silva-Ramírez, E.L. A New Insight on the Upwelling along the Atlantic Iberian Coasts and Warm Water Outflow in the Gulf of Cadiz from Multiscale Ultrahigh Resolution Sea Surface Temperature Imagery. *J. Mar. Sci. Eng.* **2024**, *12*, 1580. [CrossRef]
63. Geladakis, G.; Nikolioudakis, N.; Koumoundouros, G.; Somarakis, S. Morphometric discrimination of pelagic fish stocks challenged by variation in body condition. *ICES J. Mar. Sci.* **2018**, *75*, 711–718. [CrossRef]
64. Imre, I.; McLaughlin, R.L.; Noakes, D.L.G. Phenotypic plasticity in brook charr: Changes in caudal fin induced by water flow. *J. Fish Biol.* **2002**, *61*, 1171–1181. [CrossRef]
65. Lostrom, S.; Evans, J.P.; Grierson, P.F.; Collin, S.P.; Davies, P.M.; Kelley, J.L. Linking stream ecology with morphological variability in a native freshwater fish from semi arid Australia. *Ecol. Evol.* **2015**, *5*, 3272–3287. [CrossRef]
66. Satterfield, D.R.; Claverie, T.; Wainwright, P.C. Body shape and mode of propulsion do not constrain routine swimming in coral reef fishes. *Funct. Ecol.* **2023**, *37*, 343–357. [CrossRef]

67. Llope, M.; Anadón, R.; Viesca, L.; Quevedo, M.; González-Quirós, R.; Stenseth, N.C. Hydrography of the southern Bay of Biscay shelf-break region: Integrating the multiscale physical variability over the period 1993–2003. *J. Geophys. Res. Oceans* **2006**, *111*, C09020. [CrossRef]
68. Maestro, A.; Gallastegui, A.; Moreta, M.; Llave, E.; Bohoyo, F.; Druet, M.; Navas, J.; Mink, S.; Fernández-Sáez, F.; Catalán, M.; et al. Echo-character distribution in the Cantabrian Margin and the Biscay Abyssal Plain. *J. Maps* **2021**, *17*, 533–542. [CrossRef]
69. González-Pola, C.; Somavilla, R.; Graña, R.; Viloria, A.; Ibáñez-Tejero, L. A decade long flow reversal in the intergyre region of the eastern north Atlantic. *Prog. Oceanogr.* **2025**, *231*, 103406. [CrossRef]
70. Capoccioni, F.; Costa, C.; Aguzzi, J.; Menesatti, P.; Lombarte, A.; Ciccotti, E. Ontogenetic and environmental effects on otolith shape variability in three Mediterranean European eel (*Anguilla anguilla*, L.) local stocks. *J. Exp. Mar. Biol. Ecol.* **2011**, *397*, 1–7. [CrossRef]
71. Vaz, A.; Guerreiro, M.A.; Landa, J.; Hannipoula, O.; Thasitis, I.; Scarcella, G.; Sabatini, L.; Vitale, S.; Mugerza, E.; Mahé, K.; et al. Otolith shape analysis as a tool for stock identification of two commercially important marine fishes: *Helicolenus dactylopterus* and *Merluccius merluccius*. *Estuarine Coastal Shelf Sci.* **2023**, *293*, 108471. [CrossRef]
72. NASA Ocean Biology Processing Group. Ocean Color Data (MODIS-Aqua). Available online: https://oceancolor.gsfc.nasa.gov/ (accessed on 1 July 2024).
73. Marengo, M.; Baudouin, M.; Viret, A.; Laporte, M.; Berrebi, P.; Vignon, M.; Marchand, B.; Durieux, E.D.H. Combining microsatellite, otolith shape and parasites community analyses as a holistic approach to assess population structure of *Dentex dentex*. *J. Sea Res.* **2017**, *128*, 1–14. [CrossRef]
74. Neves, J.; Veríssimo, A.; Santos, A.M.; Garrido, S. Comparing otolith shape descriptors for population structure inferences in a small pelagic fish, the European sardine *Sardina pilchardus* (Walbaum, 1792). *J. Fish Biol.* **2023**, *102*, 1219–1236. [CrossRef] [PubMed]
75. Jurado-Ruzafa, A.; Vasconcelos, J.; Otero-Ferrer, J.L.; Navarro, M.R.; Massaro, A.; Hernández, C.; Tuset, V.M. Phenotypic response of a geographically expanding species, *Scomber colias*: Clues in the fish otolith shape. *Estuar. Coast. Shelf Sci.* **2024**, *305*, 108880. [CrossRef]
76. Spreitzer, M.L.; Mautner, S.; Makasa, L.; Sturmbauer, C. Genetic and morphological population differentiation in the rock-dwelling and specialized shrimp-feeding cichlid fish species *Altolamprologus compressiceps* from Lake Tanganyika, East Africa. *Hydrobiologia* **2012**, *682*, 143–154. [CrossRef] [PubMed]